LBL--32020

DE92 016996

Premixed Turbulent Combustion in Opposed Streams

L.W. Kostiuk and R.K. Cheng

Combustion Group
Energy and Environment Division
Lawrence Berkeley Laboratory
University of California
Berkeley, California 94720

March 1992

This work was supported by the Director, Office of Energy Research, Office of Basic Energy Sciences, Chemical Sciences Division, of the U.S. Department of Energy under Contract No. DE-AC03-76SF00098.

ABSTRACT

Premixed turbulent combustion in opposed streams has been studied experimentally by the use of two component laser doppler anemometry. This flow geometry is part of a class of stagnating flows used to study turbulent combustion in recent years. It does not involve any surface near the flames because of the flow symmetry thus circumventing many of the effects of flame surface interaction. The mean non-reacting flow is found to be self-similar for all the conditions studied in this and the stagnation plate configuration. A homogeneous region of plane straining is produced in the vicinity of the stagnation and there is a strong interaction between the turbulence in the flow and the mean straining which can increase the rms velocity as the flow stagnates. The reacting flow fields are found to be symmetric about the free stagnation point. The traverses of mean axial velocity in the stagnation streamlines for reaction flows are not dramatically different from the non-reaction flows. These results differ from turbulent combustion experiments where the flow is stagnated by a flat plate. The extinction limits was studied for propane:air mixtures.

1 INTRODUCTION

Over the past decade, reacting stagnation flows have evolved into one of the most active areas of combustion research. The reasons for this activity are primarily due to the relative simplicity of the flame and the flow geometries which lend easily to theoretical analysis and experimental interrogation.

The laminar stagnation flames are described as one-dimensional with their reaction zones subject to stretch. These laminar flames have been studied experimentally, analytically, and computationally using complex chemical kinetics. The first premixed flame configuration consisted of a uniform laminar stream stagnated by a flat plate. Due to difficulties in quantifying the effects of the plate in terms of heat loss and effects the on the chemistry, the stagnation was instead produced by an identical, opposed jet of reactants. More recently, an alternate opposed stream geometry has been used experimentally, this geometry replaces one of the reactant streams with a stream of hot products. Computational and analytical studies have used either of these opposed flow geometries. The results of these studies have contributed significantly to the understanding of the connection between aerodynamic stretching of a flame and its reaction rate, the detailed internal structure of a flame, and the processes involved in flame extinction.

Given the successes achieved by studying premixed flames in laminar stagnation flows, Cho *et al.* (1) extended the use of stagnation flows to the turbulent case. Their experiments had a uniform turbulent jet of premixed reactants stagnated by a flat plate. Though inherently more complex due to the turbulence, many of the mean attributes of the flame and the flow are preserved. A steady turbulent flame brush, which is planar in the mean, is oriented perpendicular to the jet axis and is subjected to uniform mean and fluctuating velocities over a relatively large portion of the flame area. Having a turbulent flame experiencing uniform conditions has allowed for a systematic investigation of the coupling between the turbulence and the flame. Changes to a turbulent burning velocity have been studied with respect to

the rms velocity fluctuations at the leading edge of the flame (1), and to the laminar burning velocity of the reactant mixture (2). Other studies have looked at the scale of wrinkling of the flame compared to that of turbulence (3), the details of the velocity field as the flow passes through the flame (2,4), and the observation of global flame extinction(2). The stagnation plate experiments have made a strong case for the use of a turbulent stagnation flow to study premixed combustion. The flames which exist in these flows are almost adiabatic, planar in the mean, and are subjected to a uniform velocity field[1] over much of their surface area. These features have allowed investigators to systematically alter the conditions upstream of the flame brush and observe the effects.

Under certain conditions complexities may develop if the flame is stabilized close to the stagnation plate. In this case there can be downstream heat loss if the flame is within the plate's thermal boundary layer [2], the velocity field is not as simple if the flame is within the momentum boundary layer of the plate, and the chemistry can be directly effected if the flame contacts the plate. These conditions exist when the flame is either slow burning or near to extinction. Furthermore, the plate restricts the access for measurements near to the stagnation.

The use of an opposing stream to stagnate the flow is an attempt to retain the positive features of the stagnation plate experiments, without inheriting its complexities. The opposed stream configuration with two axisymmetric premixed reactant streams is depicted in Figure 1. The absence of the solid boundary to stagnate the flow reduces the complexity of the problems by preventing heat loss from the product stream so that the chemistry of combustion is not affected. Preliminary results based on this opposed flow geometry were presented in Kostiuk *et al.* (5).

Premixed turbulent combustion in stagnating flows have been addressed theoretically by Bray *et al.* (6-8). This theory is based on a similarity transformation of the equations for continuity, momentum and progress variable prior to being solved numerically. The experimental apparatus and range of experiments described here are intended to be complimentary to these modeling efforts. Presently, the theoretical work is in three parts and considers both the stagnation plates and the opposed stream geometries. The results display many of the same features that are observed experimentally, including the possibility of extinction (6,9).

The first part of this paper examines the non-reacting opposed flow velocity field. The second part describes the reacting stagnation flow and the occurrence of extinction. The non-reacting flow results are significant for several reasons. The primary reason being that the non-reacting flow is very similar to the reactant portion of the reacting flow, and is the limiting flow field at the point of extinction of the flames. There is only a very limited amount of published work regarding the impinging of two turbulent jets. Yet, any interpretation of results of the reacting flow in terms of the velocity field upstream of the flame needs at least a qualitative understanding of turbulent stagnating jets. Also, modelers often test their models first for the case of zero heat release, which the results presented here are applicable.

The second part of the paper focuses on the velocity field with combustion and presents a mapping of the boundary where extinction occurs for lean propane:air flames. One of the principle goals of this paper is to establish the soundness of using the opposed stream

[1] Both mean and rms velocities

[2] In (3,4) the stagnation plate is made of a ceramic material and the heat loss is essentially zero.

geometry as a laboratory burner to study premixed turbulent combustion right up to the point of extinction.

2 EXPERIMENTAL SET-UP

2.1 Experimental Apparatus

The two geometrically identical burner nozzles are arranged to create a free stagnation point flow. The diameter of the nozzles are $35mm$ at their exit planes. The burner nozzles are designed to produce a uniform axial velocity profile at their exits. To keep the velocity uniform the flow within a burner nozzle is accelerated by reducing the flow area by approximately 8:1. Turbulence is generated by having perforated plates located in the flow $20mm$ upstream of the nozzle exits. To change the scale and intensity of the turbulence at the nozzle exits three different perforated plates could be used. The hole diameters in the different plates are either 2, 3, or $4mm$, and all of these plate have blockage ratios of 0.5. Downstream of the perforated plates is the exit section of the burner nozzles, which is $35mm$ in diameter and $20mm$ in length. This exit section allows the jet flows from the individual holes in the perforated plates to interact and evolve into homogeneous turbulence before leaving the burner nozzles. Generating the turbulence in this manner means that the turbulence will also be uniform across exit planes of the burner nozzles.

Air is supplied from a compressor, and its pressure is regulated to provide a steady flow to the two burners. The fuel used in these experiments is either technical grade propane or methane. The fuel and air are brought together to mix in a few meters of piping where the flow is turbulent. The mass flow rate of air or fuel are measured separately, and from this the total mass flow rate and the fuel/air equivalence ratio of the reactants supplied to the two burners is calculated. Flow rates to the individual nozzles are controlled by needle valves.

The origin of the coordinate system for measurements is placed on the mean stagnation streamline, mid-distance between the two nozzle exits. The r-axis is the radial coordinate, and the z-axis is the axial coordinate (defined as positive upward). A detailed description of the apparatus can be found in (5).

2.2 Experimental Diagnostics

To measure two components of velocity, a four-beam, two-color laser arrangement is used. Each of the two primary colors from the 4 Watt Argon-Ion laser are divided into two beams, and frequency shifted by Bragg cells. A differential frequency of $5.0MHz$ is used to remove directional ambiguity in either component. The entire laser system, optics and detectors, are mounted on a computer controlled, three-axis traversing table. Moving the probe volume within the flow is done by traversing the mounting table.

Two types of seeds are used to make velocity measurements. To follow the flow through the flame, refractory particles are introduced into the reactant stream. These particles are aluminum oxide with a nominal diameter of 3μm. This type of seed gives velocity measurements independent of whether the probe volume is in reactants, or products. These measurements are referred to as unconditional velocities. An alternate seed is a silicon oil aerosol, formed by a blasted atomizer. These oil droplets do not survive the flame, and only reactant velocities are measured. These measurements are referred to as either reactant or conditional velocities - conditioned on the state of the flow being reactants at the probe location.

Doppler bursts of scattered light resulting from particles passing through the probe volume are collected by two photomultiplier assemblies (one for each velocity component). The detectors operate in a forward scattering mode at approximately $\pm 10^{\circ}$ off the optical axis. The signal from the photodetector is amplified and filtered before the velocity of the particle that produced the burst is calculated.

At every measurement position, 8192 pairs of validated velocity data and the time between data validations are used to compute the mean and rms velocities. A pair of validated data is defined as the arrival of Doppler bursts to the two detectors within a certain time of each other. This is done to ensure that the same particle is going through both probe volumes at the same time. In this work, the criterion of validation is $10\mu s$. If the criterion is not met, then that data is ignored. Typical validation data rates are $2kHz$ in the reactant, but drops to $400Hz$ in the products due to gas expansion. The uneven volumetric seeding that exists between reactants and products means that any velocity measurement where both reactants and products are present is biased to the reactant velocity. To compensate for this uneven seeding each measurement is weighted by the time-between-data to correct back to the Reynolds averaged velocity.

The LDV system is also used to record the intermittency between reactants and products (4). When the flow is seeded with oil droplets a separate photodetector monitors the Mie scattering from the probe volume. In the products the signal is low and in the reactants the signal is high. These intermittency measurements can be used to locate the mean flame position.

3 Results and Discussion

3.1 Non-Reacting Flow

The non-reacting opposed streams are studied over the range of flow conditions found to support steady combustion. The velocity at the nozzle exit planes (W_o) has been varied from 6 to $11m/s$, the distance separating the nozzle exit planes (H) has been varied from 20 to $90mm$, and all three perforated plates have been used to generate different intensities and scales of turbulence.

The mean velocity gradients impose a bulk[3] strain rate (or bulk straining) on the flow.

[3]The choice of the word 'bulk' was used instead of 'mean' because turbulence will contribute to extensional

In a stagnation flow the straining is compressive in the axial direction, and extensional in the radial direction. For a constant density, axisymmetric flow, only one component of strain needs to be specified, and the other is fixed by continuity. In this work a bulk strain rate parameter is defined in general as

$$a_b(r,z) \equiv \frac{\partial \bar{U}(r,z)}{\partial r} \tag{1}$$

and from continuity

$$a_b(r,z) = -\left(\frac{\partial \bar{W}(r,z)}{\partial z} + \frac{\bar{U}(r,z)}{r}\right) \tag{2}$$

where $\bar{W}$ and $\bar{U}$ are the Reynolds averaged mean velocities in the axial and radial directions, respectively. Important to the nature of a stagnation point flow as a tool for studying combustion is that in the vicinity of the stagnation point a_b becomes approximately constant.

The most common means to deduce the bulk strain rate in previous turbulent stagnation flame experiments is from measurements of the mean axial velocity on the stagnation streamline. The uniformity of the flow in the radial coordinate results in

$$a_b(r=0,z) = -\frac{1}{2}\frac{d\bar{W}(z)}{dz} \tag{3}$$

A mean axial velocity traverses taken along the stagnation streamline ($\bar{W}(r=0,z)$) from one nozzle exit to the other is shown in Figure 2. Note that the mean axial velocity is not zero at the mid-point between the burners. In practise it turns out to be difficult to get the stagnation point, $\bar{W}=0$, to coincide with the $z=0$ point. This offset is caused by any small difference in flow rates from the two nozzles. Typical offset is approximately $5mm$, but with patience this can be reduced to the order of $1mm$ or less. The mean velocity, however, is symmetric about the z-plane where $\bar{W}=0$. Therefore, in terms of analyzing the data the axial distance of importance is that measured from the stagnation point which is used as the origin for all the data presented here. The gradient of axial velocity is continually changing from one nozzle to the other. At the nozzle exits (i.e. $z=-35$ and $+35mm$ in Figure 2) this gradient is small, and reaches a maximum at the stagnation point. A straight line has been used to approximate the velocity gradient in the vicinity of the stagnation point. This value of a_b near the stagnation is used as the bulk strain rate parameter to characterize the mean flow.

Self-similarity of the axial mean velocity is shown in Figure 3 contains results from four opposed stream conditions in addition to four measured previously in the stagnation plate configuration (Table 1). The stagnation plate data are shown on the left side of Figure 3. The self-similarity profiles can be expressed analytically by an error function.

A general error function to relate mean axial velocity to position can be expressed as

$$\bar{W}(z) = W_{inf}\, erf\left(\frac{z - z_{off}}{m}\right) \tag{4}$$

straining of an element in the flow, and therefore the mean straining in the flow is not the straining caused by the mean velocity gradients.

where W_{inf} is a notional velocity which the axial velocity appears to be approaching at a infinite distance from the stagnation, z_{off} is the measured offset distance between the stagnation point and the point mid-distance between the burner nozzle exits, and m is given by

$$m = -\frac{1}{\pi^{1/2}} \frac{W_{inf}}{a_b} \tag{5}$$

and scales the axial coordinate so that the slope of the velocity gradient at the stagnation will be in agreement with the slope of an error function at its inflection point.

The measured velocity data are fitted to Equation 4, and solved for W_{inf}, z_{off}, and m by the least-squared-error in velocity. The normalized velocity is then $\bar{W}(z)/W_{inf}$, and the normalized position is the argument of the error function. The data presented in these normalized coordinates in Figure 3. are for the conditions listed in Table 1.

It is important to note the hole diameter in the turbulence generator is not involved in this normalization. Therefore, the mean velocities in the central region of the turbulent stagnation flows are independent of the turbulence intensities and length scales. This describes a situation of a prescribed mean flow field acting upon the turbulence, without the feedback of the turbulence altering the mean flow.

Two other models are commonly used to describe the way the mean axial velocity varies along the stagnation streamline. Champion and Libby (10) model the axial velocity between one jet and the stagnation as

$$W(z) = \frac{4W_o z}{H}\left(1 - \frac{z}{H}\right) \tag{6}$$

and the strain rate at the stagnation becomes

$$a_1|_{W=0} = \frac{2W_o}{H} \tag{7}$$

Williams (11) infers a linear change in axial velocity and models the strain rate at the stagnation to be

$$a_2|_{W=0} = \frac{W_o}{H} \tag{8}$$

Values of a_1 and a_2 for the four opposed flow conditions shown in Figure 3 have been calculated and added to Table 1. Our data shows that the model of Williams (11) always underestimates the bulk straining, while the parabolic model of Champion and Libby (10) provides a better estimate but overestimates when the nozzle separation is small and underestimates when the separation is large.

The self-similarity of the velocity profiles allows the bulk strain rate near the stagnation to be estimated more precisely from W_o and H. This is particularly useful when detailed velocity measurements are not available and for this purpose the concept of an effective nozzle separation (H_{eff}) is used. The bulk strain rate is then calculated by

$$a_b = \frac{W_o^+ - W_o^-}{2H_{eff}} \tag{9}$$

where W_o^+ and W_o^- are the nozzle exit velocities of the individual nozzles. From measurements over the range of experimental conditions, the effective separation can be functionally related to the physical separation. The distances over which the the effects of the stagnation are felt (i.e. H_{eff}) is believed to scale with the jet diameter and beyond that separation the strain rate in not strongly effected by changing the separation. The equation relating H and H_{eff} can be generalized by using separations normalized by the nozzle diameter which would make these results applicable to flows created by other jet diameters.

The relationship between the physical and effective separations also gives some insight into the physics of opposed streams. For large nozzle separations the structure of the mean flow around the stagnation is independent of the nozzle separation, and for a set nozzle exit velocity there is a minimum strain that exists at the stagnation. This highlights the main problem with models given in (10,11) is that they infer that the nozzle separation is inversely proportional to the strain rate for a given nozzle exit velocity.

The rms velocities for the opposed flow configuration along the stagnation streamline are shown in Figure 4. Both the axial ($w'(r = 0, z)$) and the radial ($u'(r = 0, z)$) rms velocity traverses have the same general features. The turbulence initially decays, falls to a minimum, and then increases to a local maximum at the stagnation. Therefore, as a result of the flow stagnating and the plane strain (bulk straining) applied to the fluid, there is a mechanism for increasing the turbulent kinetic energy in the flow. For the axial rms velocity, the regions of decay and increase roughly coincide with the regions of low and high strain rates, respectively. The radial rms velocity continues to decay for a longer time than the axial component and its increase appears less dramatic than the axial component. Throughout the entire traverse the corresponding Reynolds stress is essentially zero.

The joint probability density functions (jpdf) of U and W for selective points around the stagnation point, are also shown in Figure 4. At the two points nearest the free stagnation point the jpdf is slightly bimodal in the W velocity. The primary and secondary peaks of the jpdf are built around velocities of opposite signs. This form of jpdf suggests that the data has been collected at a point where the flow has had two different mean velocities (and of different signs). One explanation for this observation is that the interface between the two jets is shifting or bouncing around in this region of the flow on a time scale longer than the turbulence time scale. This would mean that data was collected intermittently from one jet and then from the other jet. An alternate explanation is that the particles used for the LDV measurements are unable to follow the flow in these highly strained regions and they cross from one jet to the other. In either event the magnitude of the axial rms velocity for the points in the immediate vicinity of the stagnation are made larger by this phenomena.

To further understand the mechanism of the rise in rms velocity the data has been plotted in a different form in Figure 5. Plotting in this form allows for the deviation from normally decaying turbulence in a free stream to be seen more clearing. The insert in Figure 5 shows the normal decay in axial rms velocity generated from the $3mm$ hole diameter perforated plate in a free jet. In this form, normal decay is a straight line of positive slope - negative slope would indicate an increase in the turbulence. The line represented this normal decay has been transferred to the main part of Figure 5 to allow for comparison with data from one of the streams in the opposed jet configuration. The effects of the straining is first noticed in the axial component of the rms velocity. The deviation from the normal decay of turbulence occurs almost as soon as the mean velocity begins to slow down. The effects on the radial

velocity do not occur until much nearer the stagnation. These results show that the primary mechanism of increasing the turbulence in the flow is done through velocity fluctuation in the axial direction. The change in the radial rms may in fact be due to a transfer of turbulent kinetic energy from the axial component where it is produced to the radial component.

4 Reacting Flows

4.1 General Flame Features and Extinction

The twin flames produced by the opposed stream burner are circular in shape and are approximately $80mm$ in diameter. They are wrinkled by the turbulence, but appear planar in the mean. Under typical stable burning conditions, the flames are separated about the stagnation point. The flow conditions, however, can be adjusted so that the two flames move closer together. At some point the flames are so close that they visually appear as a single flame. The appearance of one reaction zone represents a weak burning condition, and the flames are approaching global extinction. The changes in physical parameters that move the flames together are : decrease in nozzle separation, increase nozzle exit velocity, increase in turbulence intensity, or change in fuel:air mixture away from stoichiometric. Unlike the laminar stagnation flames no non-planar flames have been observed in the turbulent case.

For a given equivalence ratio (ϕ) there is a limited range of conditions that combustion can be stabilized. At higher flow rates and higher turbulence levels, the flames can extinct. No matter which of the physical parameters of the experiments is changed to cause extinction, the approach towards global extinction is always the same. The two flames move closer together until they visually appear as a single reaction zone, their luminosity decreases, and then suddenly the flames disappear. Sometimes just prior to extinction the flames spend a few seconds going partially extinct and then restabilizing before global extinction occurs.

The global extinction boundary of the opposed flames can be mapped in terms of the mean axial velocity at the nozzle exit ($W_{o,E}$), nozzle separation (H_E), equivalence ratio (ϕ_E), and hole diameter in the turbulence generator (d_E), where the subscript E is reminder that these are values at extinction. The procedure used to force the flames to extinction is as follows. The burners are well separated when the flow is ignited. The flow rates of fuel and air are then adjusted to a desired $W_{o,E}$ and ϕ_E. The burners are then slowly moved closer together until global extinction occurs. The separation distance at which extinction occurred (H_E) is recorded along with the other physical parameters at extinction.

Extinction experiments were only done for lean propane-air mixtures. Figures 6 shows the extinction boundary for the conditions stated on the individual figures. The scatter in the data points that form the extinction boundary appear to come from two main sources. (1) turbulent extinction is a statistical event, and does not occur at the same point each time, and (2) uncertainty in the measurement of ϕ_E, as extinction is *very* sensitive to equivalence ratio. The relative positions of the extinction boundary shows the effects of changing equivalence ratio or the perforated plate. The extinction boundary is shifted upwards for equivalence ratios nearer to stoichiometric and for perforated plates with smaller holes. Comparing the extinction boundary of $\phi_E = 0.8$ and $\phi_E = 0.9$ with $d_E = 3mm$, shows that mixtures nearer

to stoichiometric are capable of reaction at higher flow rates (approximately $2m/s$ or 30% higher) for a given nozzle separation. This indicates that mixtures nearer to stoichiometric are more robust, and can withstand larger rates of bulk straining and more intense turbulence before extinction occurs.

4.2 Reacting Flow Field

The mean axial velocity traverse are examined for two quite different flow conditions. The first of these is a propane:air flame far from extinction $W_o = 7m/s$, $H = 55mm$, $d = 3mm$ and $\phi = 0.9$ propane, and the second is a methane:air flame near to extinction. The unconditional Reynolds mean axial velocity traverse of the propane:air flame is shown in Figure 7. This mean velocity traverse has been inverted about the $\bar{W} = 0$ point, and overlaid on itself to show the symmetry about the free stagnation point. In terms of mean velocities there is no difference between the upper and lower streams, even during combustion, though buoyancy forces do affect the positioning of the stagnation.

The remarkable feature of this mean velocity traverse is how subtle an effect combustion has on the shape of the traverse when compared to the non-reacting flow Figure 2. Despite the large temperature rise caused by the combustion, and the resulting dilation of the gasses occurring at near atmospheric pressure, there is no large increase in the magnitude of axial velocity. There is simply a slower deceleration of the flow in the axial direction through the central part of the flame brushes.

Both Cho *et al.* (1) and Lui and Lenze *et al.* (3) use the minima in the unconditional mean axial velocity as a measure of the turbulent burning velocity. The idea being that this minima is caused by heat release near the leading edge of the flame brush, and may be considered to be a representative propagation velocity of the turbulent flame. This definition of a burning velocity cannot be used for the opposed streams results presented here, because a minima in axial mean velocity often does not exist. An alternate burning velocities would be to define the burning velocity in terms of the mean axial flow velocity at a chosen mean progress variable ($\bar{c}$) from the intermittency measurements. It should be noted that either of these definitions of a turbulent burning velocities are arbitrary.

The mean axial velocity traverse of a methane:air flame near to extinction is shown in Figure 8. The reason for analyzing a flow near to extinction, is to compare its mean axial velocity traverse with the non-reacting case, and to verify that - as extinction is approached, the reacting flow field approaches the non-reacting flow field.

The line drawn in Figure 8 has been calculated from the self-similar profiles found from the non-reacting flow of the same nozzle separation and nozzle exit velocity. There is very little difference between the near extinct and the non-reacting mean velocity traverse. This similarity justifies the use of non-reacting results to approximate the bulk strain rate of a flow just upstream of the flames at the point of extinction.

The rms velocity in both the axial and radial directions for the propane:air flame are shown in Figure 9. There is little difference between the conditional and unconditional data in either the axial or radial component. Unlike the mean axial velocity traverse, the traverse

of axial rms changed more dramatically from the non-reacting case. The traverse of axial rms velocity shows an initial decay in the rms velocity, followed by a small increase, but then instead of continuing to rise as in the non-reacting case there is further decay through the flame brushes before finally rising steeply to a maximum rms velocity at the stagnation. In interpreting the non-reacting results, the connection was made between the changes in the axial rms velocity and the local bulk strain rate. It is worth noting that the regions of decay in axial rms velocity are also the regions of relatively low bulk strain rate is small and regions of increasing rms velocity are associated with large straining. In contrast to the axial rms velocity, the radial rms velocity traverse is essentially unchanged for the non-reacting case.

Included in Figure 9 are three joint pdf's of the axial and radial velocities for the unconditional velocity measurements. The only joint pdf of interest is the one closest to the stagnation point as the form of this pdf is distinctly bi-modal. This bi-modal feature was also found in the non-reacting flow very near the stagnation with the two peaks of the pdf having opposite signs. It is believed that this is a result of either *bouncing* of the stagnation point or the seed particles unable to follow the flow in these large gradients in mean velocity. As with the non-reacting flow it should be emphasized that this behavior is limited to a region very near the stagnation. Data collected $1mm$ further away from the stagnation shows no sign of a bi-modal pdf.

These sets of results are very different from the stagnation plate experiments of Cho *et al.* (4), and Lui and Lenze (2). The dominant feature of their rms velocity traverses is the large increase in axial rms velocity in the flame brush. By sampling from reactants and products as the flame crossing the measurement volume, a large axial rms velocity is calculated. The large rms velocity is not production of turbulence by the flame, but simply the result of combining two velocity distributions with different means. In the opposed streams this large difference in reactant and product mean velocities at a single point does not exist. Therefore, the large rise in unconditional axial rms velocity was not to be expected in the opposed streams. The reason for the difference between the opposed streams and the stagnation plate experiments is the large difference in the bulk straining (see Table 1.

Using the same seeding as for the conditional velocity measurements, the intermittency between reactants and products is measured. Intermittency is defined here as the fraction of time a point in the flow spends in products. Defined in this way, the intermittency is equivalent to the Reynolds averaged progress variable ($\bar{c}$).

A traverse of the intermittency, or $\bar{c}$, for the propane:air flame is shown in Figure 10. The data points where $\bar{c} = 0$ are positions in the flow where only reactants are ever present. Since $\bar{c}$ never reaches unity, there is no place on the stagnation streamline in this particular flow where products gasses are only present. From these results the mean position of the flame brush can be deduced and interpreted back onto the velocity traverses as in Figure 7. The distribution of $\bar{c}$ is roughly symmetric about the maxima of the $\bar{c}$, which also corresponds with the stagnation point. This indicates that the upper and lower fames are similar despite the effects of buoyancy and one flame being a hot-over-cold interface and the other being a less stable cold-over-hot interface.

5 CONCLUSIONS

An experimental study of the velocity field in turbulent, opposed streams with and without combustion has been presented. The non-reacting results provide a general characterization of turbulent stagnation flows for the interpretation of the results obtained in reacting flows.

The burners were designed for the flow to be axisymmetric, and the mean and rms velocities are independent of the radial coordinate in a central core of the jets. LDV measurement between the two nozzles along the stagnation streamline shows that the mean velocity field is symmetric about the free stagnation plane. This symmetry in velocity field does not extend to the turbulent velocities, unless the flow rates from the two nozzles are made absolutely equal.

The mean non-reacting velocity field is found to be similar for all nozzle exit velocities, nozzle separations, and turbulence generators tested. This allows the mean axial velocity traverses to be normalized, so that all the measured data in the opposed stream configuration and those obtained previously in stagnation plate configuration all lies on the same curve. The shape of this is self-similarity profile is adequately expressed as a error function.

The flames produced in these experiments are circular in shape, and approximately $80mm$ in diameter. In the mean, the flames appear flat and perpendicular to the axial coordinate. Hence, the mean flame position is independent of the radial coordinate. Therefore, a large portion of the turbulent flame brush in the opposed stream geometry is experiencing the same upstream conditions. Intermittency measurements of progress variable show the two flame brushes to be similar and symmetric about the free stagnation point.

Traverses of mean axial velocity on the stagnation streamline are not dramatically different from the non-reacting flow. There is no large increase in axial velocity as the flow crosses the flame. These results differ from turbulent combustion experiments where the flow is stagnated by a flat plate.

Under certain conditions, the flames can be forced to extinction, and this limit to turbulent combustion was studied for lean propane:air mixtures. For flames that are near to extinction there is very little measured difference in the mean axial velocity, when compared to the non-reacting results. This similarity between near extinct and non-reacting flows allows results of extinction experiments to be interpreted from velocity information collected from the non-reacting case.

ACKNOWLEDGEMENTS

The authors would like to thank Prof. K.N.C. Bray and Dr. I.G. Shepherd for their useful comments and discussions throughout all stages of this work. Support for this work is gratefully acknowledged - the work of LWK at the University of Cambridge: Natural Sciences and Engineering Research Council of Canada and The Edmonton Churchill Foundation, for RKC: Director, Office of Energy Research, Office of Basic Energy Sciences, Chemical Sciences Division of the U. S. Department of Energy under Contract No. DE-AC-03-76SF00098.

REFERENCES

1. Cho, P., Law, C.K., Hertzberg, J.R., and Cheng, R.K. *Twenty-First Symp. (Int.) on Comb.*, The Comb. Inst., 1986, pp1493-1499.
2. Liu, Y. and Lenze, B. *Twenty-Second Symp. (Int.) on Comb.*, The Comb. Inst., 1988, pp747-754.
3. Shepherd, I.G., Cheng, R.K., and Goix, P. *Twenty-Third Symp. (Int.) on Comb.*, The Comb. Inst., 1990, pp781-787.
4. Cho, P., Law, C.K., Cheng, R.K., and Shepherd, I.G. *Twenty-Second Symp. (Int.) on Comb.*, The Comb. Inst., 1988, pp739-745.
5. Kostiuk, L.W., Bray, K.N.C., and Chew, T.C. *Combust. Sci. and Technol.*, 64:233-241 (1989).
6. Bray, K.N.C., Champion, M, and Libby, P.A. *Combust. Flame*, 84:391-410, (1991).
7. Bray, K.N.C., Champion, M, and Libby, P.A. *Submitted for Publication.*
8. Bray, K.N.C., Champion, M, and Libby, P.A. *Submitted for Publication.*
9. Bray, K.N.C., Champion, M., Kostiuk, L.W., and Libby, P.A. *Seventh Symp. on Turbulent Shear Flows*, Stanford University, 1989, pp1.2.1-1.2.6.
10. Champion, M. and Libby. P.A. *To appear in Phys. of Fluids*
11. Williams, F.A. *Fire Safety J.* 3:163-175 (1981).

Table 1: Physical Parameters of Experiments Shown in Figure 3

Condition	$W_o(m/s)$	$H(mm)$	$d(mm)$	$H_{eff}(mm)$	$a_b(s^{-1})$	$a_1(s^{-1})$	$a_2(s^{-1})$
Opposed	6.7	70	3	32.8	205	191	96
Opposed	8.7	55	2	32.2	270	316	158
Opposed	8.4	20	2	15.3	550	840	420
Opposed	11.1	70	4	32.8	338	317	158
Plate	4.9	53	4.5	29	84	-	-
Plate	4.1	53	4.5	40	53	-	-
Plate	5.5	103	4.5	51	54	-	-
Plate	6.9	103	4.5	43	81	-	-

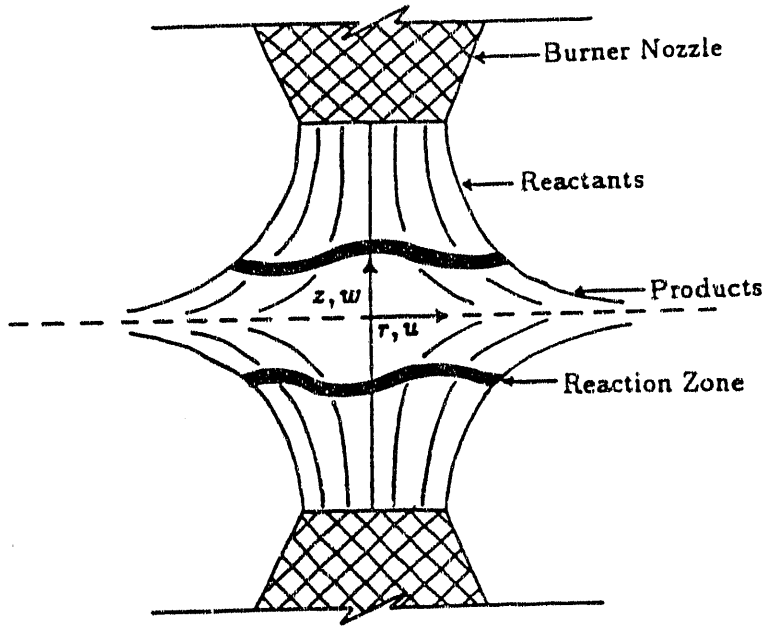

Figure 1 Schematic of Experimental Apparatus.

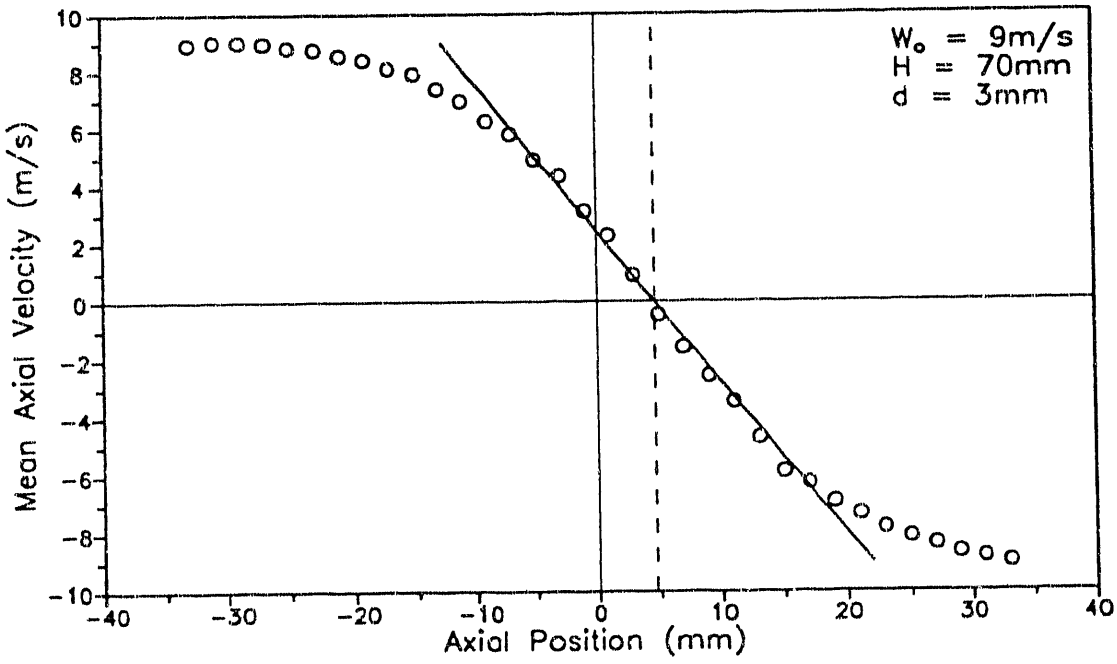

Figure 2 Mean Axial Velocity Traverse in Non-Reacting Flow.

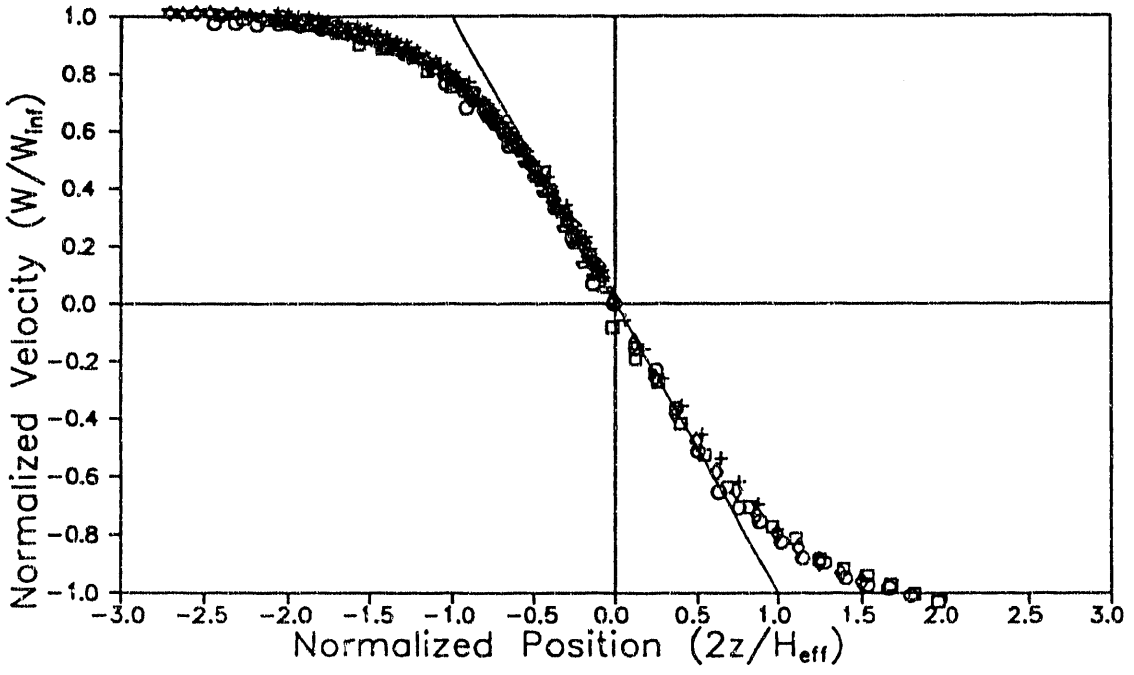

Figure 3 Normalized Mean Velocity Traverses in Non-Reacting Opposed Streams and Stagnation Plate Flows.

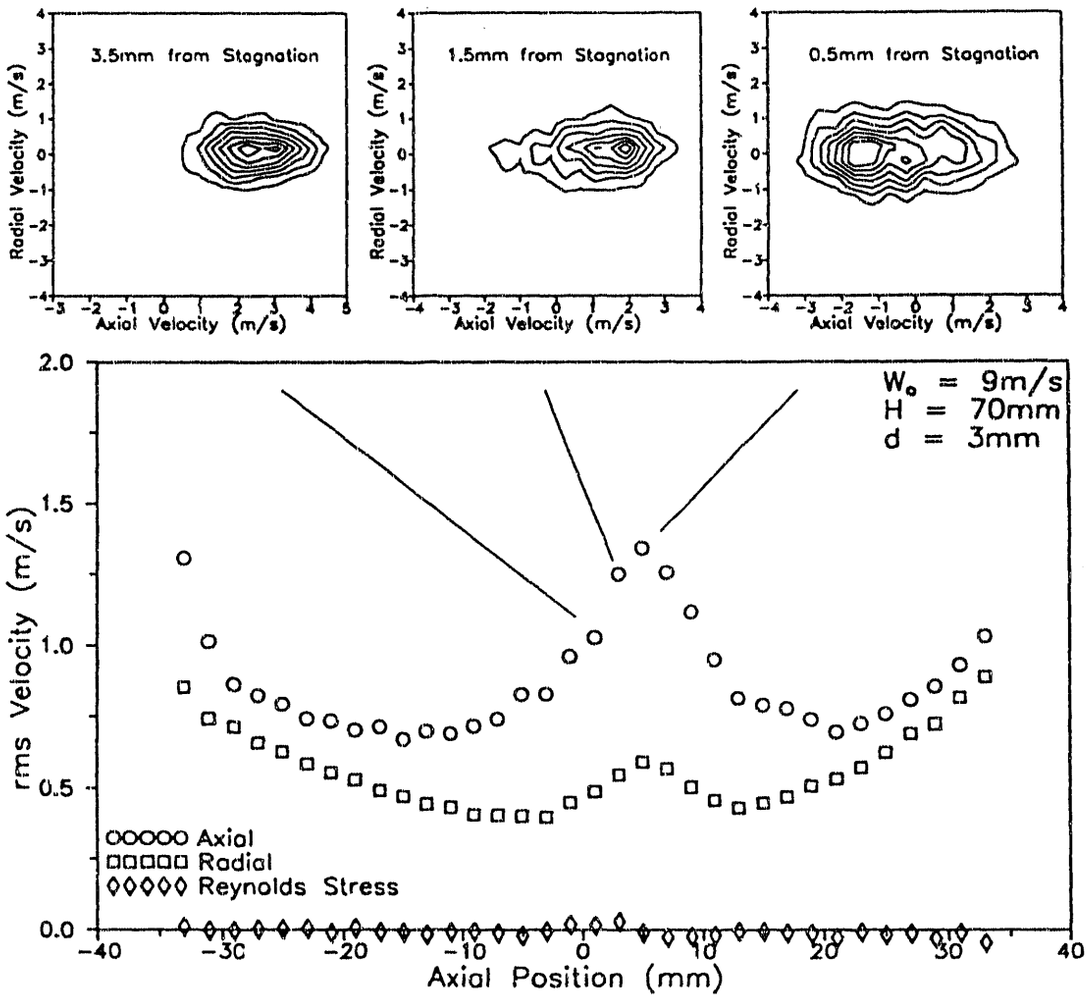

Figure 4 Axial and Radial rms Velocity Traverse in Non-Reacting Flow.

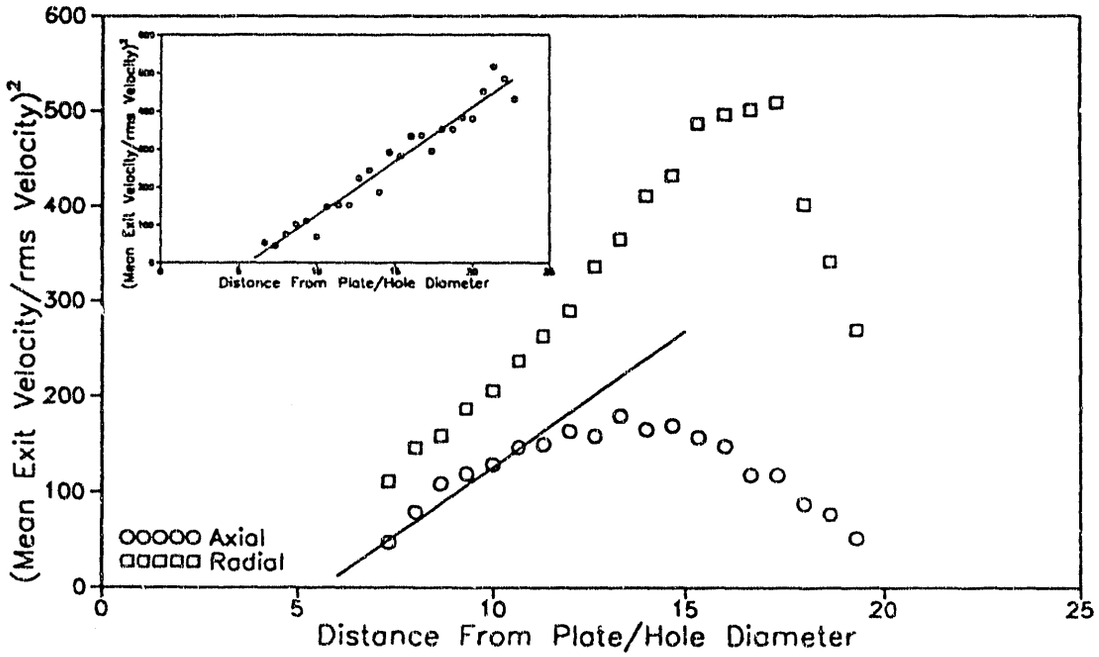

Figure 5 Evolution of Turbulence in Non-Reacting Flow.

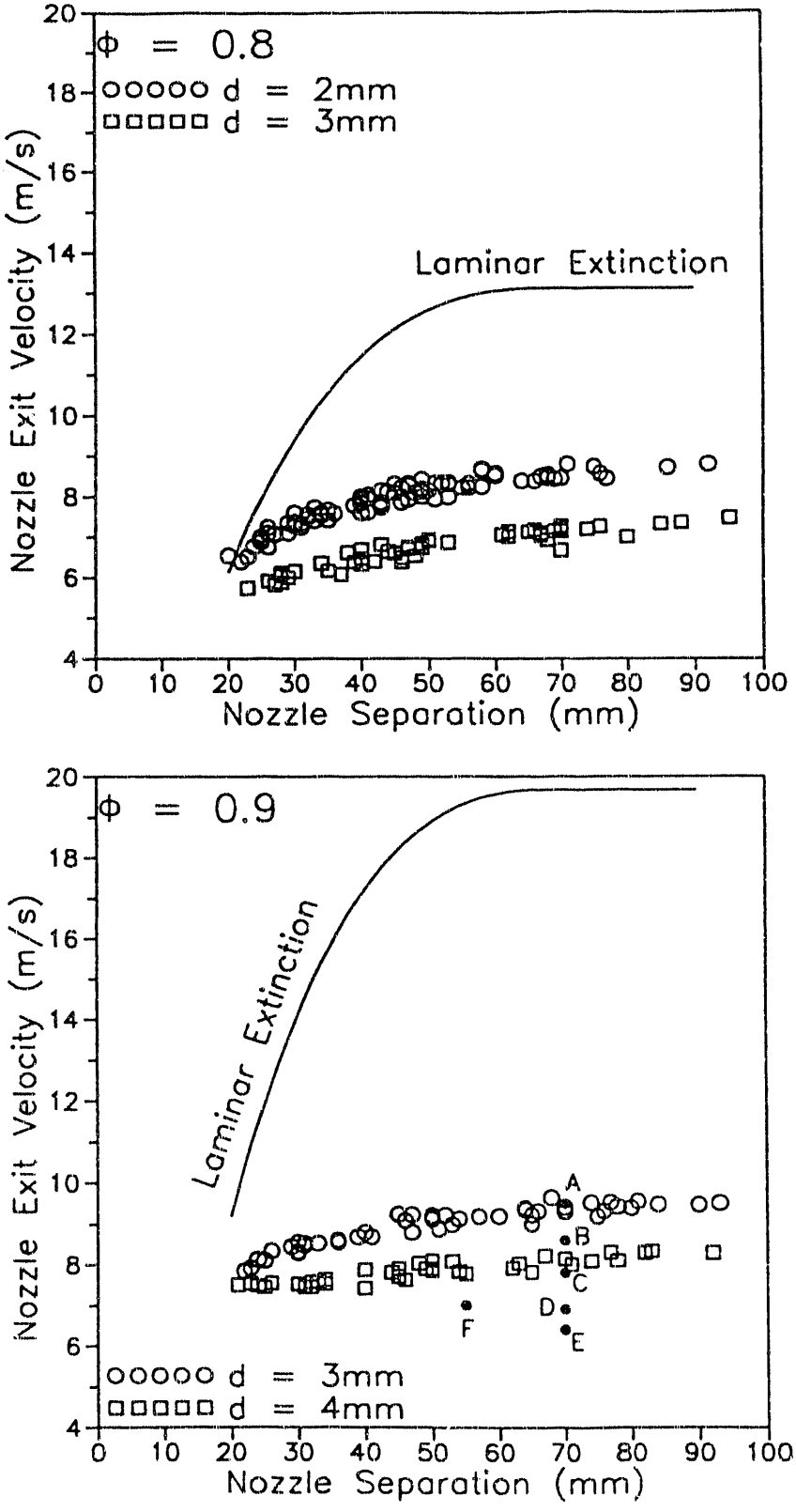

Figure 6 Extinction Boundary for Propane:Air Flames.

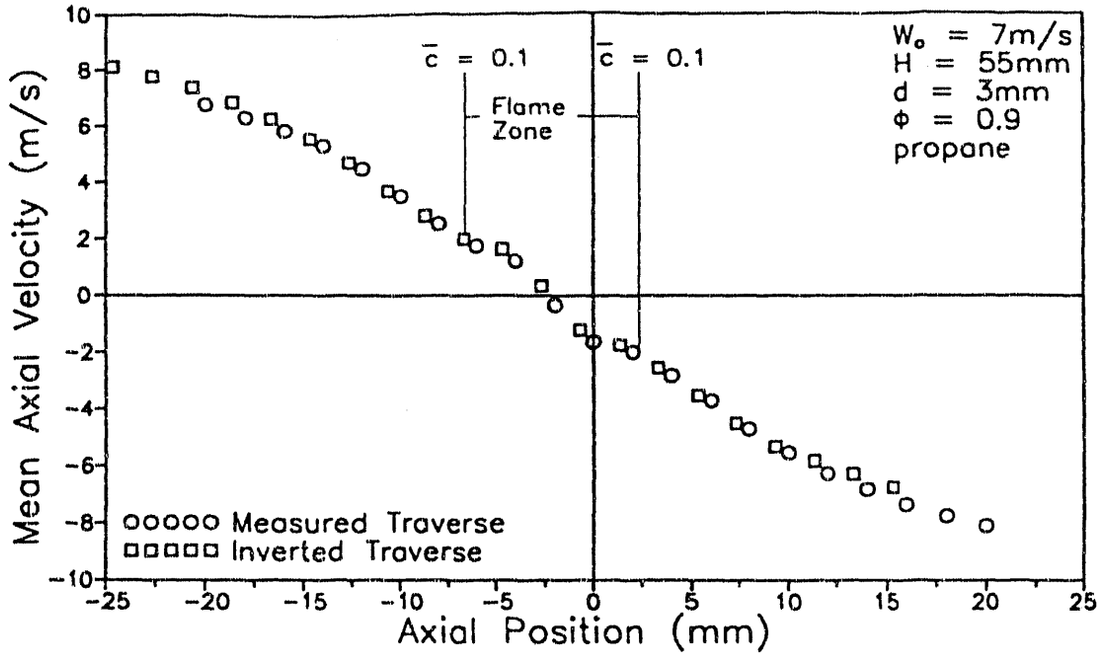

Figure 7 Unconditional Mean Axial Velocity Traverse in Reacting Flow.

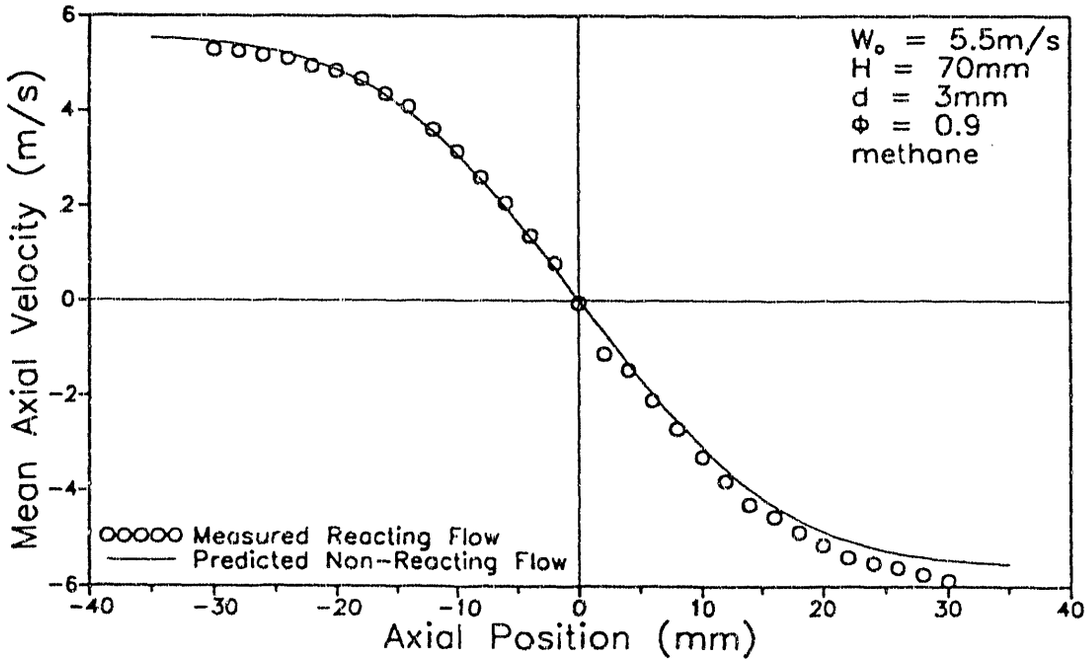

Figure 8 Unconditional Mean Axial Velocity Traverse of Methane:Air Flames Near Extinction.

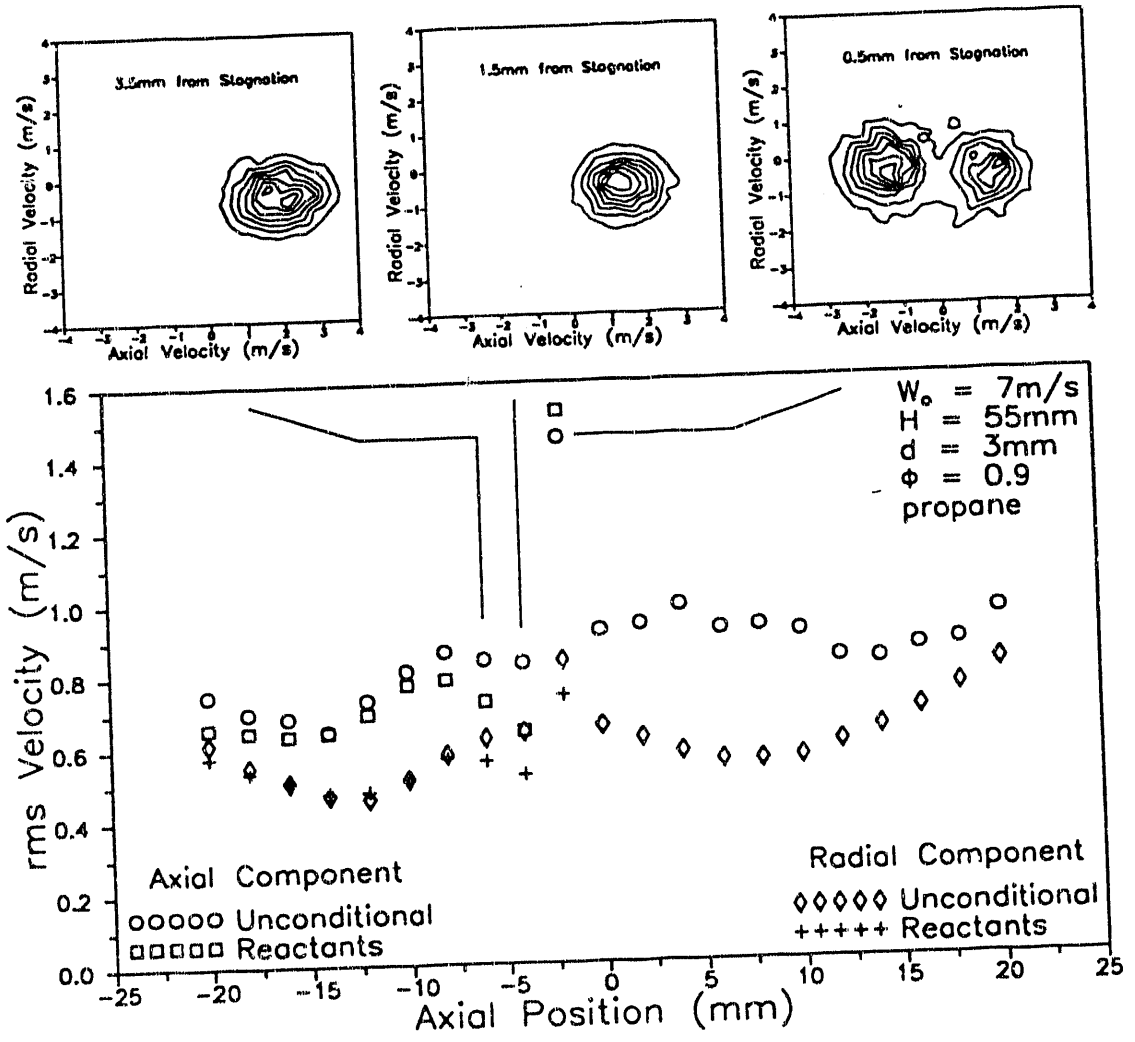

Figure 9 Axial and Radial rms Velocity Traverse in Reacting Flow.

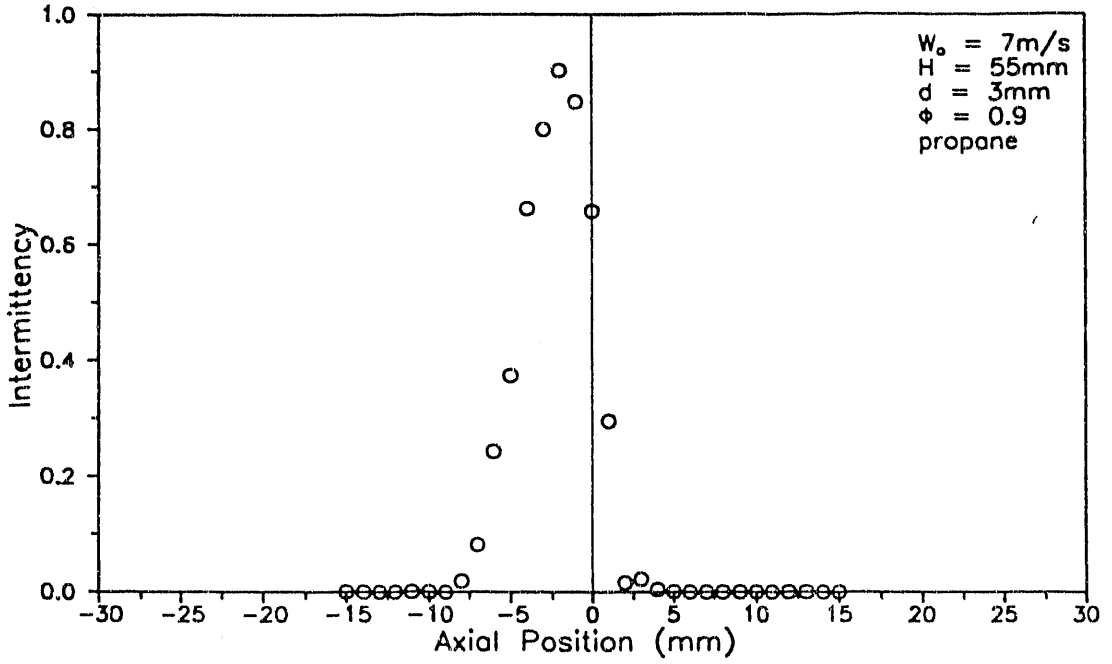

Figure 10 Intermittency Traverse.

END

DATE FILMED

8/20/92